

Paper:

Design of A Hybrid Transmission Line Inspection Robot

Xiaoyu LONG*, Guodong YANG**, En LI**, Zize Liang**

*School of Artificial Intelligence, The University of Chinese Academy of Science, No. 19, Yuquan Road, Shijingshan District, Beijing

**Institute of Automation, Chinese Academy of Science, 95 Zhongguancun East Road, 100190, Beijing, China

E-mail: longxiaoyu2019@ia.ac.cn, guodong.yang@ia.ac.cn, en.li@ia.ac.cn, zize.liang@ia.ac.cn

[Received ; accepted]

Abstract. A hybrid transmission line inspection robot is a combination of a multirotor and a power line landing mechanism, which can perform both airborne and on-wire inspections. An improved design of a hybrid automatic inspection system is demonstrated in this paper, planned to land on a shield line. Installed with a lightweight landing mechanism consists of a belt system drive linear motion mechanism and a gear rack drive wire clamber, the robot can perform both airborne and on-wire inspection to powerlines. The finite element analysis on key components was conducted. In the field, the robot was found to have an acceptable flight performance.

Keywords: Powerline Inspection Robot; Robot Components Design

1. Introduction

Due to the unbalanced distribution of electricity resources among our country, [5], a large scale of transmission apparatuses has been established among geographically diverse and climate varied terrain. In these areas, power transmission lines and apparatus may be eroded by natural factors, superimposing by the material nature of powerlines, different types of line damage are prone to occur[12], which may lead to a power outage. To prevent these accidents, it is necessary to conduct regular inspections to find hidden dangers and possible faults that endanger the safety of power transmission. The inspection work of transmission lines is still mainly manual method, which has greater personnel risk and high time cost[4]. Improving the level of line inspection automation is important to ensure the safe operation of transmission lines and in face of the increasing labor cost.

In this paper, we present the design of a hybrid transmission line Inspection robot combining a multirotor and a wheel-based landing mechanism, being able to land on a shield wires. The mechanism consists of the linear motion mechanism and the wire clamber. The former allows the whole UAV platform to slide along the designated line. The wire clamber is used to apply extra grips on the line, giving the whole platform a stable moving performance on the line. Due to the loading capability of

the selected multirotor, strict weight constrain is applied to the whole landing system. Eventually, this system is controlled through an open-sourced flight control board: Pixhawk 4, which provides control functionalities on both flight control and landing mechanism control.

2. Related Works

The research on electric powerline inspection robots can be traced back to the 1980s[1], aiming at robots used in harsh operating environments such as nuclear power plants, highways, and power transmission lines in Europe and the United States, and other countries. In the field of power inspection, the focus of relevant researches at home and abroad is focused on the research and development of small-sized autonomously movable robots[6]. For instance, [9] designed a two-arm electric inspection robot that installs return-springs being able to move along the line continuously, and it can surpass the counterweight dampers and splicing sleeves on wires. But the robot cannot pass obstacles such as warning balls and suspension of anti-vibration hammers. LineScout robot[8] is equipped with two extra robotic arms that are used as grippers to assist the robot to cross obstacles. When crossing obstacles, they respectively grasp and fix the two ends of the obstacle to be crossed, and then the robot body passes through the obstacle through the linear track under the two mechanical arms using linear pushing. The idea of landing an aerial robot on the power line was traced back to Jones. D and Golightly's work on the concept design of a small, ducted-fan rotorcraft[3]. But its relocation performance is unsatisfactory since it cannot lift to an acceptable height from the wire. Hydro-Quebec developed a hybrid line inspection robot for internal flaw detection of high-voltage lines[7] that also has a low center of gravity, and a special wrapping mechanism for detecting wires is placed between the two wheels in the middle of the body. The aircraft rely on remote control to complete landing tasks at high altitudes, which is relatively difficult to accomplish. [10] come up with a design of a walking mechanism mounted on the top of the multirotor platform. [2] have developed a hybrid robot prototype having a lower open hopper chassis is installed at the bottom of a UAV. The robot can safely land on the target line of the power transmission network and slide through

a custom-designed landing gear. It uses a carriage is to assist passive positioning of the ground line during landing.

3. Mechanical Structure of the Hybrid Robot

3.1. Design of the Mechanical Structure

As demonstrated in Fig.1, to achieve required inspections on wires, insulators, and other electrical components, our hybrid robot consists of a multirotor drone and a landing mechanism with battery packs mounting on landing gears. The landing mechanism is installed at the bottom of the multirotor, and the battery pack installed at the bottom of the drone landing gear to lower the center of gravity, and other mechanical components of the robot are set symmetrically under the consideration of placing the center of gravity project on the centerline of the robot.



Fig. 1. The overview of the hybrid robot

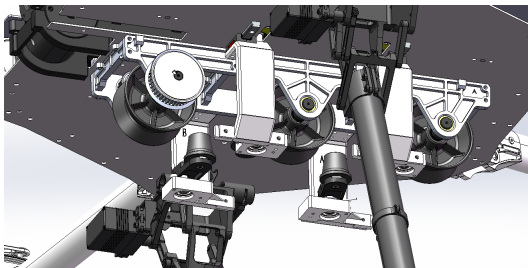


Fig. 2. The overview of the hybrid robot's landing mechanism

As shown in Fig.2, the linear motion mechanism is a single-line three-wheel structure, powered by a brushless DC motor. The selection of the motor is based on the operational velocity and the sliding friction between wheels and the surface of the cable[11], mounting above the sliding mechanism. The motor is installed with its axis of the shaft coincides with the robot's centerline, hence an extra gearbox with a pair of helical gears is designed and mounted on the motor. The power is imported to a syn-

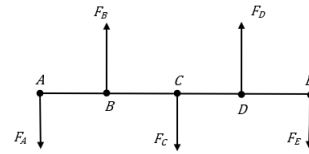


Fig. 3. The Force analysis of the landing wire

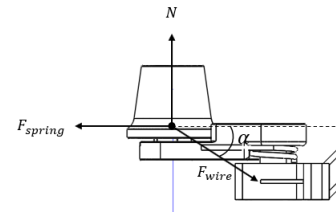


Fig. 4. The Force analysis of the clamp wheel

chronous belt hence each wheel can be driven by the synchronous belt wheel system.

the clammer mechanism is designed to combine four clamping arms with a link linkage device as each clammer arm is installed on the linear rail mounted on the base as shown in. Meanwhile, a rotary arm with a designated torsion spring, mounting at its pivot, is installed on each clamping arm to generate clamping force when the wire gripping is enforced and a support wheel having a rounded bottom is placed at the end of it.

As shown in Fig.3, it is assumed that the wire at the landing location is an ideal straight line, then 3 identical vertically downward forces and 4 identical upward forces are exerted on the wire by wheels and clamps respectfully. In term of the force and moment equilibrium, the following equations can be established:

$$F_A + F_C + F_E - 2(F_B + F_D) = 0 \quad \dots \dots \dots (1)$$

$$F_C l_{AC} + F_E l_{AE} - 2(F_B l_{AB} + F_D l_{AD}) = 0 \quad \dots \dots (2)$$

$$F_A = F_C = F_E = N_{wheel} \quad \dots \dots \dots (3)$$

$$F_B = F_D = 2N_{clamp} \quad \dots \dots \dots (4)$$

$$3N_{wheel} + 4N_{clamp} = G_{robot} \quad \dots \dots \dots (5)$$

Hence, according to the force scheme of a clammer wheel Fig.4, the force exerted by the torsion spring is:

$$F_{spring} = \frac{N_{clamp}}{\tan \alpha} \quad \dots \dots \dots (6)$$

Based on this result, the diameter of the torsion spring can

be determined as the following:

$$d_{spring} = \sqrt[3]{\frac{32T_n K_1}{\pi \sigma_{Bp}}} \dots \dots \dots (7)$$

$$\sigma_{Bp} = 0.8 \sigma_b \dots \dots \dots (8)$$

$$K_1 = \frac{4C - 1}{4C - 4} \dots \dots \dots (9)$$

$$T_n = F_{spring} l_{arm} \sin \beta \dots \dots \dots (10)$$

Subscribing parameters in Table.3.1 to equations above, the diameter of the torsion spring is calculated to be 1.4 mm.

Table 1. Parameters of the torsion spring selection

Parameters	Unit	Value
G_{robot}	N	28.91
σ_b	MPa	2150
l_{AB}	mm	57.5
l_{AC}	mm	115
l_{AD}	mm	172.5
l_{AE}	mm	230
l_{arm}	mm	30
α	deg	26
β	deg	22
C		10

The whole clammer system is powered by the motor having the same configuration as that utilized in the sliding mechanism so that the equilibrium along the robot’s longitudinal direction can be maintained. While a gear rack system is utilized to the power transmission of the clammer system, with a spur installed on the output shaft and the rack mounted on the linkage device. The linkage device is connected to the base via two parallel linear rails on it while shafts on clamping arms are placed in the sliding grooves. Hence the clammer system realizes the synchronizing clamping movements of all the holding arms are obtained through these sliding grooves laying on the link linkage device.

3.2. On-wire Stability Analysis of the Robot

The robot is mainly stabilized by the battery bundles hanging on each landing gear. As the weight of the whole system has to be controlled stringently, which should not exceed the maximum take-off mass of the multirotor: 5kg, the height of the wheel mounting location has to be calculated for on-wire balance. The schematic diagram of the robot’s lateral section can be established as shown in Fig.5.

In this diagram, it is assumed that the centroid of the robot frame is located at point F, while battery packages are hanged on the point A and B separately. Edge CD represents the base of the multirotor, and landing gears are represented as edge AD and BD, and the robot’s wheels contacts with a wire at point G. To maintain the lateral stability at an arbitrary pose, the equilibrium between the acting moment and the residual moment on the lateral section must be achieved, where point G is the pivot. Given the critical situation is that the robot will not fall from

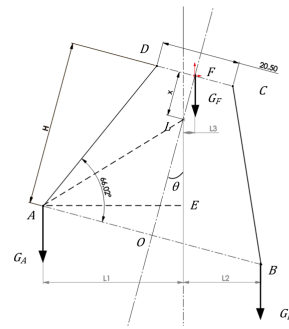


Fig. 5. Force diagram on the lateral direction of the robot

the wire or hang upside-down when the angle of the centerline against the vertical, θ , reaches 15 degrees. Then following equations can be established to figure out the distance x :

$$G_A L_1 \geq G_B L_2 + G_F L_3 \dots \dots \dots (11)$$

$$L_1 = l_{AL} \cos \alpha, \alpha = \angle OAL \dots \dots \dots (12)$$

$$\alpha = \arctan \left(\frac{l_{OL}}{l_{OA}} \right) \dots \dots \dots (13)$$

$$L_2 = (l_{OB} - l_{OL} \tan \theta) \cos \theta \dots \dots \dots (14)$$

$$L_3 = x \sin \theta \dots \dots \dots (15)$$

Meanwhile, x should not less than the largest radius of the wheel, which is 30 mm, hence the offset from the base is calculated using the numerical method with constraints mentioned above. Parameters are demonstrated in the following table:

Table 2. Parameters of the line stability analysis

Parameters	Unit	Value
G_A	N	28.91
G_B	N	28.91
G_F	N	98.44
l_{OA}	cm	27.15
l_{OB}	cm	27.15
l_{OF}	cm	49.5
θ	deg	15

With the parameters given above, the numerical result of the distance LF , from the wheel center to the robot base, is calculated to be 44.5 mm.

3.3. Simulations of key parts

To control the weight of the whole system, the landing part is mainly constructed using aluminum alloy. There are mainly two types of key parts: the power shaft and the clammer arm where the former is directly connected with the motor and carries the robot line movement, the latter one exerts compression to the wire. Their simulation results are shown in follow figures:

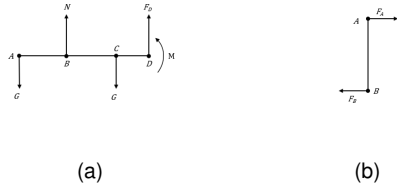


Fig. 6. Force analyses of the power shaft (a) and the clamper arm(b)

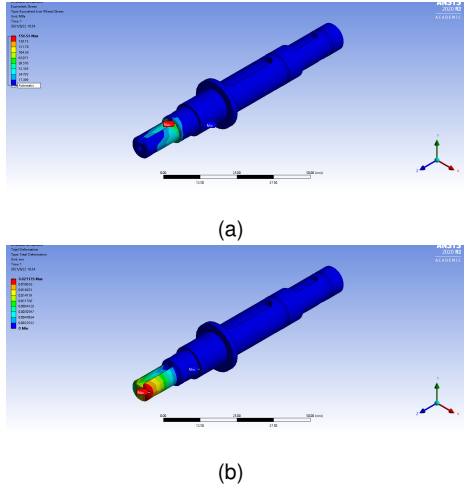


Fig. 7. Simulation result of the power shaft: the stress simulation (a), the deformation simulation (b)

The force analysis of the power shaft is demonstrated in Fig.3.3(a), where N is the normal force from the wire, G is the robot weight distributed at the shaft, F_D and M are the belt tension force and motor torque respectively. As shown in Fig.7(a), the maximum value of von-Mises stress occurs at the transition edge from the thinnest segment to the medium one and the value turns out to be 156.54 MPa. The deformation result is illustrated in Fig.7(b). The maximum deformation appears at the tip of this segment, which is 0.021 mm.

Clamper arms exert extra grips to the wire, whose force analysis is shown in Fig.3.3(b),and their simulation result are illustrated in Fig.8. The maximum value of the equivalent stress occurs at the transition segment of the slider rod, located at the top of the arm, which is 163.12 MPa. The maximum deformation locates at the bottom part, and the value is 0.7848 mm. Above all, these key parts are satisfied with the force requirement of the landing mechanism.

4. System Overview

The control system structure is demonstrated in Fig.9. The high-level controller is selected to be NVIDIA Jetson TX2, while an open-source flight control unit(FCU): Pixhawk 4, is chosen to be the flight controller as well

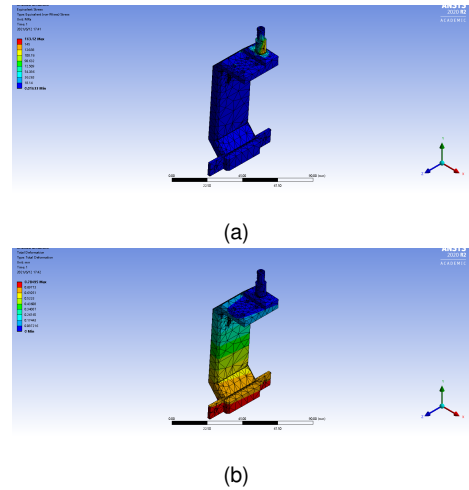


Fig. 8. Simulation result of the Clamper arm: the stress simulation (a), the deformation simulation (b)

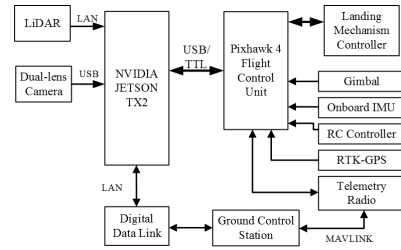


Fig. 9. Control System Structure of the Robot

as the landing mechanism controller. A LiDAR and a dual-lens camera are connected with TX2 who are mainly used for mapping and the line-inspection target identification. These data streams are processed on TX2 and sent to FCU through MAVROS protocol, hence information from the high-level controller such as targets' poses. Also, information on FCU such as IMU readings can be sent to TX2 via this protocol. The landing mechanism can be controlled directly via an RC controller as well as MAVROS off-board nodes running on TX2, achieving the function of landing in both manual and automatic methods. A ground control station is set to communicate with TX2 and FCU via a digital data link and a telemetry radio separately so that both video streaming and flight data inspection can be obtained by the operator on a laptop ground station.

5. Test Result

The hybrid robot prototype, as shown in Fig.10, based on this design was tested in the field to examine the effect of the current layout on its flight performance. The robot vibration on its poses is estimated in terms of Ac-



Fig. 10. Test Flight of the robot

tuator Controls FFT and Power Spectral Density of the robot acceleration. The former mainly describes the actuator's control signal frequencies on the roll, pitch, and yaw axis and the latter is the frequency response of the raw accelerometer data against time, all of which are illustrated in Fig.11. According to Fig.5, there is a vibration having a peak at 30Hz on the roll axis, which could cause by battery packs on landing gears. This can be also observed in Fig.5 around this frequency. Such a vibration was observed in the flight as a obvious but decreasing oscillation when there was a control input on the roll axis. Except that, the rotor flight performance is relatively acceptable since vibrations on other directions are considerably low.

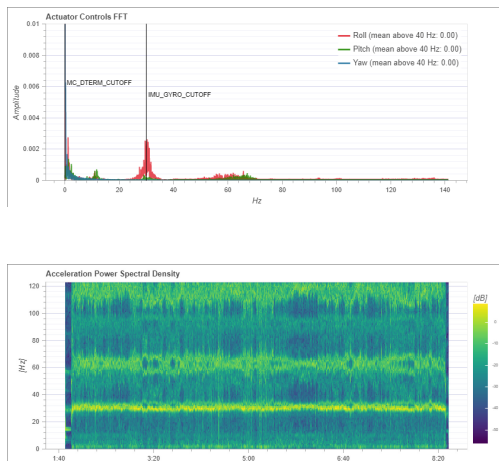


Fig. 11. Actuator Controls FFT(a) and Acceleration Power Spectral Density on the robot orientation(b)

6. Conclusion

We have presented a design of the hybrid transmission line robot being able to achieve both airborne and on-wire inspection of the power grid via multiple sensors

including visual sensors, LiDAR. An improved landing mechanism has both durability and light-weight that allows the robot to perform both flying mode and on-wire mode inspection. The structure of the robot is optimized under consideration the natural structure of a multicopter and loading capability hence the landing mechanism can be integrated organically to ensure both flight safety as well as sliding stability on the shield wire. Also, several key parts has been testified via numerical static simulation method on. Further works on this robot are planned to achieve the fully automatic inspection on wires through several methods, including visual methods, point clouds methods, etc. In addition, the fine-tune flight pose control on the roll axis is to be achieved to granted flight stability during the inspection.

Acknowledgements

Project "Research on Key Technologies of Inspection Robots for Overhead Transmission Lines" supported by the National Natural Science Foundation of China (No.U1713224, No.61973300)

References:

- [1] A. B. Alhassan, X. Zhang, H. Shen, and H. Xu, "Power transmission line inspection robots: A review, trends and challenges for future research", *International Journal of Electrical Power and Energy Systems*, 118:105862–, 2020.
- [2] W. Chang, G. Yang, J. Yu, Z. Liang, L. Cheng, and C. Zhou, "Development of a power line inspection robot with hybrid operation modes", In 2017 IEEE/RSJ International Conference on Intelligent Robots and Systems (IROS), pp. 973–978, 2017.
- [3] I. Golightly and D. Jones, "Visual control of an unmanned aerial vehicle for power line inspection", In ICAR '05. Proceedings., 12th International Conference on Advanced Robotics, 2005., pp. 288–295, 2005.
- [4] W. Li, "Risk Assessment of Power Systems: Models, Methods, and Applications", 2004.
- [5] J. Liu, D. Niu, and X. Song, "The energy supply and demand pattern of China: A review of evolution and sustainable development", *Renewable and Sustainable Energy Reviews*, 25(1):220–228, 2013.
- [6] L. Matikainen, M. Lehtomaki, E. Ahokas, J. Hyyppa, M. Karjalainen, A. Jaakkola, A. Kukko, and T. Heinonen, "Remote sensing methods for power line corridor surveys", *Isprs Journal of Photogrammetry and Remote Sensing*, 119:10–31, 2016.
- [7] F. Mirallès, P. Hamelin, G. Lambert, S. Lavoie, N. Pouliot, M. Montfrond, and S. Montambault, "LineDrone Technology: Landing an Unmanned Aerial Vehicle on a Power Line", In 2018 IEEE International Conference on Robotics and Automation (ICRA), pp. 6545–6552, 2018.
- [8] N. Pouliot, P. Latulippe, and S. Montambault, "Reliable and intuitive teleoperation of LineScout: a mobile robot for live transmission line maintenance", In 2009 IEEE/RSJ International Conference on Intelligent Robots and Systems, pp. 1703–1710, 2009.
- [9] Y. Song, H. Wang, and F. Jing, "Obstacle performance analysis for a novel inspection robot with passive joints", In 2011 IEEE International Conference on Robotics and Biomimetics, pp. 926–931, 2011.
- [10] X. Tan, Z. Yi, R. Yuan, and Z. PU. "Multi-rotor aircraft used and the power line inspection system based on it", 2015.
- [11] H. Wang, E. Li, G. Yang, and R. Guo, "Design of an Inspection Robot System with Hybrid Operation Modes for Power Transmission Lines", In 2019 IEEE International Conference on Mechatronics and Automation (ICMA), 2019.
- [12] F. Zhou, A. Wu, Y. Li, J. Wang, and Z. Liang, "Development of a mobile robot for high voltage overhead power transmission lines", *Automation of Electric Power Systems*, 28(23):89–91, 1 2004.